

EREM 81/1Journal of Environmental Research,
Engineering and Management

Vol. 81 / No. 1 / 2025

pp. 35–43

10.5755/j01.erem.81.1.36557

The Effect of Particle Size, Activation Type and Contact Time of Cocoa Pod Husk (*Theobroma Cacao* L.) Activated Carbon on Artificial Waste Chromium Adsorption Capability

Received 2024/04

Accepted after revisions 2024/12

<https://doi.org/10.5755/j01.erem.81.1.37115>

The Effect of Particle Size, Activation Type and Contact Time of Cocoa Pod Husk (*Theobroma Cacao* L.) Activated Carbon on Artificial Waste Chromium Adsorption Capability

Ari Fernando Panjaitan, Eva Eklesia Sitanggang, Henokh Sitorus, Vikram Alexander, Rondang Tambun*

Department of Chemical Engineering, Faculty of Engineering, Universitas Sumatera Utara, Indonesia

***Corresponding author:** rondang@usu.ac.id

Cocoa (*Theobroma cacao* L.) is among the top commodities in Indonesia but the economic value is only limited to seeds, and pod husk is considered a waste. Cocoa pod husk contains cellulose, hemicellulose, and lignin, suggesting great potential as activated carbon. In this study, the cocoa pod husk activated carbon used varied in various sizes, namely particles passing through a 20 mesh sieve and retained by a 40 mesh sieve (20/40), particles passing through a 50 mesh sieve and retained by a 70 mesh sieve (50/70), particles passing through a 90 mesh sieve and retained by a 120 mesh sieve (90/120), and particles passing through a 150 mesh sieve and retained by a 200 mesh sieve (150/200). The carbon was then chemically activated using 0.8 M phosphoric acid (H_3PO_4), soaked for 8 hours, and physically activated using an oven at 110°C for 1 hour. The activated carbon was contacted with chromium (Cr(VI)) for 6 hours, 12 hours, and 24 hours. The results showed that, based on the atomic absorption spectroscopy test, the best Cr(VI) adsorption occurred in the adsorbent with a 150/200 mesh particle size variation, which chemically activated with a contact time of 24 hours. The adsorbed Cr(VI) content was 992.02 ppm with an adsorption efficiency of 99.20%. Correspondingly, an iodine number test of 850.23 mg/g was obtained on activated carbon with a particle size of 150/200 mesh, which was chemically activated. The scanning electron microscope analysis results showed a porous, rough, and distributed activated carbon surface.

Keywords: activated carbon, adsorption, artificial waste, cocoa pod husk, chromium.

Introduction

Environmental pollution by heavy metals is a great concern for the public due to the adverse effects worldwide (Briffa et al., 2020). The indiscriminate discharge of industrial wastewater harms the natural environment due to rapid development. Heavy metal wastewater is the most hazardous among many aquatic industrial wastes. An example of heavy metals highly ranked after lead (Pb(II)) and mercury (Hg(II)) as environmental pollutants from industrial activities is chromium (Cr(VI)). Sources of chromium entering the environment include industrial activities such as cement, paint, steel, textile, leather, ceramic, and paper factories. According to previous reports, it enters the human body through soil accumulation and plant contamination (Adiloğlu and Göker, 2021). Given the toxic nature, the Environmental Protection Agency (US EPA) stipulates that industrial effluent must contain less than 0.5 mg/L of the Cr(VI) before being discharged into the environment. The limit for the Cr(VI) in drinking water must be less than 0.05 mg/L (Georgaki and Charalambous, 2023).

Proper treatment of heavy metal waste is crucial to avoid polluting the environment. Some methods used for treatment include remediation with surfactants (Haryanto et al., 2023), biosurfactants (Chen et al., 2020), and adsorption with physical and chemical activation. Adsorption is an effective purification method to remove hazardous metal ions from polluted water (Kuroki et al., 2019). The three basic stages of adsorption into a (solid) adsorbent include pollutant movement from the aqueous solution to the surface, adsorption, and transportation within the particles (Chai et al., 2021). The adsorption process is still the preferred method due to the high effectiveness, easy procedure, simple recovery, wide adaptability, high efficiency, and economy. Additionally, the adsorbent is recycled numerous times, and potentially harmful effects of adsorbent material degradation can be removed (Mizhir et al., 2022; Hasanpour and Hatami, 2020). In recent years, a variety of adsorbents, including porous inorganic materials, organic materials, and biological materials, have been used to trap heavy metal ions (Mei et al., 2023). The adsorption process is selected for use in various industrial separation chemical processes due to the economical assessment. This method uses adsorbent and adsorbate which can be in gaseous (Mudoj et al., 2022) and liquid phase (Mishra et al., 2023).

The most often used adsorbent is activated carbon (Noble and Terry, 2004) due to high adsorption capacity, large surface area, polymodal (but fundamentally microporous) porous structure, and changing surface chemical composition (Rodríguez-Reinoso, 2001). Other advantages of activated carbon as an environmentally friendly adsorbent include the capacity to withstand high temperatures, chemical stability, resistance to strong acids and bases, effective adsorption capabilities, ability to be made from various raw material sources, and easy regeneration (Wang et al., 2022). A previous study by Waly et al. (2021) examined the adsorption process of Pb(II) and Hg(II) metal ions using water hyacinth-activated carbon. The results showed high adsorption capacity to remove Pb(II) and Hg(II) up to 310.9 mg/g and 252.5 mg/g, respectively, at a temperature of 298 K, pH of 5.5, and stirring for 60 minutes from an adsorbate concentration of 800 ppm. In a study conducted by Kakom et al. (2023), activated carbon from the pyrolysis of bagasse was used to adsorb heavy metals such as manganese (Mn) from the initial concentration of 0.2503 mg/kg to 0.0840 mg/kg at a contact time of 20 minutes. The amount of activated carbon used was 2.5 g and a mass of 20 g adsorbate at a temperature of 34°C, with 1 atm. Another study by Brishti et al. (2023) used activated carbon from *Bombax ceiba* fruit peel to adsorb heavy metal iron (Fe(III)) in an aqueous solution. The percentage of Fe(III) removed was 99.10% from the initial concentration of 75 mg/L to 0.675 mg/L with a contact time of 25 minutes, an adsorbent dose of 0.05 g/25 mL of 75 mg/L Fe(III) solution, and pH conditions of 3.5. Furthermore, Naboulsi et al. (2024) used composite beads of activated carbon/sodium alginate (CA/Alg) prepared from a *Retama Monosperma* (L.) Boiss plant as adsorbent for pesticide 2,4,5-trichlorophenoxyacetic acid batch adsorption. The results showed effective removal rates, achieving 84.08% at a concentration of 80 ppm, pH = 2, and a contact time of 1650 minutes (Naboulsi et al., 2024). A study by Rabichi et al. (2024) on olive mill solid waste biochar for vanillic acid adsorption correlated well with the pseudo-second-order and Langmuir models. The maximum adsorption capacity was $q_m = 57.47$ mg/g and the correlation coefficient was $R^2 = 0.999$ (Rabichi et al., 2024). Bouzid et al. (2024) optimized Eriochrome Black T adsorption through in-situ polymerization of poly(aniline-co-formaldehyde) on biochar and obtained an exceptional adsorption capacity of 700.01

mg/g (Bouزيد et al., 2024). Based on the results of previous studies, it is necessary to vary the use of other natural materials as an alternative source of activated carbon. Potential natural materials include agricultural or food industry waste, which is the largest contributor to organic waste presently. Therefore, to solve this problem, it is necessary to use agricultural and food industry organic waste to reduce the amount of existing waste (Meftah et al., 2024). One of the organic wastes that can be used as raw material for making activated carbon is cocoa pod husk (*Theobroma cacao* L.).

A significant component of Indonesian economy is cocoa, which is considered one of the top strategic plantation commodities (Herawati et al., 2023). Based on World Population Review data, the third-largest producer of cocoa in the world is Indonesia with a total production of 659 776 metric tonnes (World Population Review, 2022). The cocoa fruit consists of 75% skin and 25% seeds, which are the main raw material for chocolate production (Fang et al., 2020). The economic value of cocoa fruits lies only in the seeds, while pod husks are a waste that has limited use as fertilizer and animal feed (Budaraga and Putra, 2020). Cocoa pod husk contains 21.06% of hemicellulose, 51.98% of lignin, and 20.15% of cellulose (Yuli et al., 2021). The waste has a great potential as an adsorbent in solving the problem of water pollution by heavy metal and other polluting wastes due to the high carbon elements. In this study, artificial Cr(VI) metal waste was adsorbed by cocoa pod husk activated carbon that had been activated first, and then the impact of the particle size on the adsorption ability of cocoa pod husk activated carbon was evaluated.

Methods

Materials

The materials used in this study were cocoa pod husks sourced from Parangan Village, Simalungun District, Sumatera Utara Province, Indonesia, aquadest, Cr(VI) artificial waste 1000 ppm Uni-Chem brand, phosphoric acid (H_3PO_4) 0.8 M Merck brand, starch indicator Merck brand, iodine 0.1 N Merck brand, and sodium thiosulfate ($Na_2S_2O_3$) 0.1 N Merck brand.

Equipment

The equipment used in this study included atomic absorption spectroscopy (AAS) type GBC AVANTA A6506,

aluminum foil, mesh sieve sizes of 20 mesh, 40 mesh, 50 mesh, 70 mesh, 90 mesh, 120 mesh, 150 mesh, and 200 mesh RLS brand, ball mill, beaker glass, glass funnel, desiccator, erlenmeyer, furnace, filter paper, magnetic stirrer, digital balance Vernier brand type VE-B2000C with a 0.01 g accuracy, oven Memmert brand, and scanning electron microscope (SEM) type JSM 6510 Series.

Preparation of cocoa pod husk as activated carbon

Cocoa pod husks were cleaned with water to remove any remaining dirt, then cut into pieces measuring 2 cm x 2 cm x 1 cm, dried in the sun for 7 days, and baked in an oven for 30 minutes at 80°C to eliminate the moisture content. Subsequently, carbonization was carried out using a furnace at 300°C for 30 minutes, followed by grinding using a ball mill and filtration to obtain the sample size of 150/200 mesh, 90/120 mesh, 50/70 mesh, and 20/40 mesh. The sample size of 150/200 mesh implies the particles passing through a 150 mesh sieve and retained by a 200 mesh sieve, the sample size of 90/120 mesh means the particles passing through a 90 mesh sieve and retained by a 120 mesh sieve, the sample size of 50/70 mesh means the particles passing through a 50 mesh sieve and retained by a 70 mesh sieve, and the sample size of 20/40 mesh means the particles passing through a 20 mesh sieve and retained by a 40 mesh sieve.

Physical activation

Activated carbon with particle size variations of 150/200 mesh, 90/120 mesh, 50/70 mesh, and 20/40 mesh was placed into an Erlenmeyer, activated by heating with an oven at 110°C for 1 hour using an oven, and then the steam was removed in a desiccator.

Chemical activation

Activated carbon with particle size variations of 150/200 mesh, 90/120 mesh, 50/70 mesh, and 20/40 mesh was chemically activated by soaking it in a 0.8 M phosphoric acid (H_3PO_4) solution (Matsedisho et al., 2024) for 8 hours. Subsequently, filtration was carried out using filter paper, and the activated carbon was washed with aquadest.

Chromium adsorption

Activated carbon of 15 g with particle size variations of 150/200 mesh, 90/120 mesh, 50/70 mesh, and 20/40

mesh that had been physically activated was placed into an Erlenmeyer, and then 1000 ppm of the Cr(VI) artificial waste liquid was added. The Erlenmeyer was closed using aluminum foil, left, then stirred with a magnetic stirrer at a speed of 400 rpm and variations in contact time of 6 hours, 12 hours, and 24 hours. The procedure was also carried out for chemically activated carbon.

Pore surface description analysis of activated carbon

The surface description for cocoa pod husk activated carbon pores was analyzed using the magnification method before and after adsorption, while the tool used was SEM.

Test of adsorbed chromium level

The Cr(VI) content adsorbed by activated carbon was obtained from testing the content in the adsorbate before and after the adsorption process, while the tool used was AAS.

Iodine number test

Activated carbon of 0.25 g that had been activated was placed into an Erlenmeyer, then 25 mL of 0.1 N iodine solution was added. The mixture was then agitated for 15 minutes before being left to stand. This was followed by filtration using filter paper, and the filtrate of 10 mL was pipetted and titrated with 0.1 N sodium thiosulfate ($\text{Na}_2\text{S}_2\text{O}_3$) until the mixture turned pale yellow. Titration was performed again after adding 3 drops of a 1% amyllum indicator until the mixture turned colorless. The iodine number can be calculated with *equation (1)* (Yuliusman et al., 2020).

$$\text{Iodine number} = \frac{(10 - ((B \times C)/D)) \times 12.69 \times Fp}{W} \quad (1)$$

where C is the normality of a standardized sodium thio-phosphate solution (0.1 N); D is the normality of iodine solution (0.1 N); W is activated carbon mass (0.25 g); B is a required amount of a sodium thiosulfate solution (mL); 12.69 is the amount of iodine equivalent to 1 mL of 0.1 N iodine solution; Fp is the ratio of iodine solution required to that titrated (25 mL/10 mL).

Chromium adsorption analysis

Adsorption efficiency was obtained based on data from the AAS test. This test aimed to obtain data on the adsorbate final concentration value after adsorption,

then the data were used to calculate the adsorption efficiency based on *equation (2)* (Khit et al., 2023), while the adsorption capacity was calculated based on *equation (3)*.

$$\text{Adsorption efficiency (\%)} = \frac{(C_0 - C_e)}{C_0} \times 100\% \quad (2)$$

$$\text{Adsorption capacity} = \frac{C_0 - C_e}{m} V \quad (3)$$

where C_0 is adsorbate concentration before adsorption (ppm); C_e is adsorbate final concentration after adsorption (ppm); m is the amount of the adsorbent (g); V is the volume of the solution (mL).

Results and Discussion

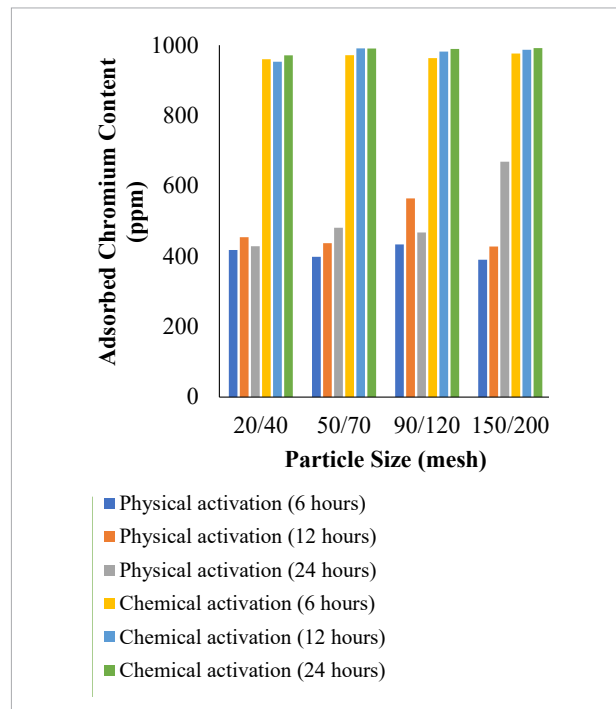
Effect of activation type, particle size, and contact time of activated carbon on adsorption capability

The effect of activation type, particle size, and contact time on adsorption ability is shown in *Fig. 1*.

Fig. 1 shows that the activation of chemically activated carbon produced more Cr(VI) adsorption ability than physically activated carbon at all variations of contact time and particle size. At a contact time of 6 hours, the best particle size to adsorb Cr(VI) was chemically activated 150/200 mesh, which removed up to 976.26 ppm. In the chemically activated carbon, there were fluctuations in particle size 90/120 mesh, while in physically activated carbon, there were fluctuations in particle size 50/70 and 150/200 mesh. At a contact time of 12 hours, the best particle size to remove Cr(VI) was chemically activated 50/70 mesh which removed up to 991.04 ppm. Data fluctuations occurred in chemically activated carbon at a particle size of 90/120 mesh, while in physically activated carbon, fluctuations occurred at particle sizes 50/70 and 150/200 mesh. At a contact time of 24 hours, the best particle size to remove Cr(VI) was chemically activated 150/200 mesh, which removed up to 992.02 ppm. Chemically and physically activated carbon activation data both fluctuated at the 90/120 mesh particle size.

In general, an increase in the Cr(VI) adsorption rate occurred with decreasing particle sizes of activated carbon. The maximal bed capacity and breakthrough time were demonstrated to decrease as the adsorbent particle size increased. Smaller particles have shorter diffusion pathways, allowing the adsorbate to reach deeper

Fig. 1. Effect of activation type, particle size, and contact time of activated carbon on adsorbed chromium content



more quickly, and increase in the particle size; hence, it takes less time to reach saturation. This is because the reduction in the adsorbent surface area caused by bigger particle sizes leads to fewer active sites for absorption. Greater surface area for adsorbate and adsorbent interaction is represented by smaller particle sizes. The removal efficiency, saturation time, adsorption capacity, and volume of treated effluent all increased. Larger particle sizes have a reduced adsorption capacity; hence, more area will be needed to accomplish high mass transfer (Andrade et al., 2022). Similar results were obtained in a study by Arslan et al. (2022) on the adsorption process of Cr(IV) metal ions using leonardite powder. The particle size with the highest adsorption efficiency was 45 μm , which adsorbed Cr(IV) metal ions by 63.8%, while the 300 μm particle size only absorbed 47.6%. The surface area of activated carbon to adsorb Cr(VI) increases with the decreasing particle size.

The best activation to adsorb more Cr(VI) based on Fig. 1 is the chemical type. The results showed that the Cr(VI) content adsorbed by chemical activation was higher compared with physical activation for all adsorbent particle size variations. This is because chemical activation provides high adsorbent surface area, better

porosity (Husien et al., 2022), a simple process, and a better activation effect compared with physical activation (Hsiao et al., 2023). Sakhiya et al. (2021) also conducted a comparative study on the chemical and physical activation of rice straw biochar to improve the adsorption process of zinc metal ions (Zn(II)). The results showed that chemical activation can increase the total volume of pores and specific surface area approximately twice and three times higher respectively compared with physical activation.

Iodine number analysis

The iodine number results for cocoa pod husk activated carbon calculated using equation (1) are presented in Table 1.

Table 1. Iodine number test of cocoa pod husk activated carbon

Particle Size (mesh)	Activation Type	Iodine Number (mg/g)
20/40	Chemical	494.91
	Physical	444.15
50/70	Chemical	799.47
	Physical	507.60
90/120	Chemical	824.85
	Physical	571.05
150/200	Chemical	850.23
	Physical	634.50

The best iodine number of 850.23 mg/g was obtained using the chemically activated carbon with a particle size of 150/200 mesh. Based on the results, the smaller the particle size, the higher the iodine number value. Generally, a high iodine number denotes a high rate of adsorption on activated carbon. The high adsorption rate suggests that activated carbon has a large surface area and pore volume (Mercileen et al., 2023). High adsorption rates are produced as the adsorbent particle size decreases (El Nemr et al., 2022). This implies that the activated carbon with the smallest particle size had the highest iodine number. Although physical activation also increases the iodine number, the effect is less pronounced compared with chemical activation. Physical activation usually entails thermal treatment, which drives off volatile components and creates porosity, but it may not achieve the same degree of pore development as chemical activation (Heidarinejad et al., 2020). The iodine numbers for physically activated adsorbents

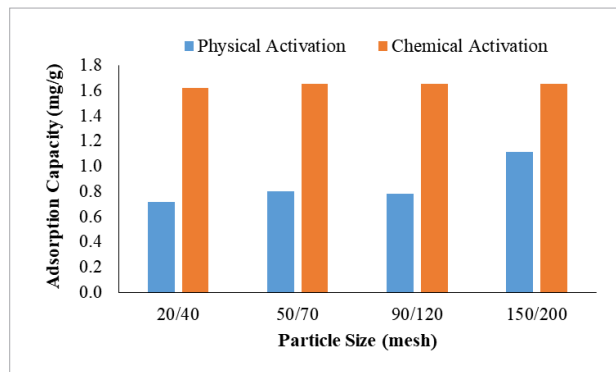
were consistently lower, indicating reduced micropore development.

Adsorption capacity analysis

The results of adsorption capacity analysis for cocoa pod husk activated carbon are presented in Fig. 2.

Fig. 2 shows the analysis of adsorption capacity using activated carbon from cocoa pod husk for adsorbed Cr (VI) content. The highest adsorption capacity obtained was 1.653 mg/g with chemically activated carbon from cocoa pod husk. The results showed that the adsorption capacity values generally increased with larger particle sizes for both activation methods. This observation could be attributed to the larger surface area available for adsorption in the larger particle size (Bouzidi et al., 2021). Across all particle size ranges, chemically activated adsorbents consistently outperform the physically activated counterparts. The superior performance of chemical activation can be attributed to the ability to enhance adsorbent affinity toward the target adsorbate (Mariana et al., 2021). Chemical activation often induces more microporosity, which contributes to higher adsorption capacity by improving chemical bonding (Chimi et al., 2023). The consistently higher adsorption capacity values for chemically activated samples, regardless of a particle size, suggest that activation type plays a more dominant role in adsorption efficiency than particle size.

Fig. 2. Adsorption capacity analysis of activated carbon on adsorbed chromium content



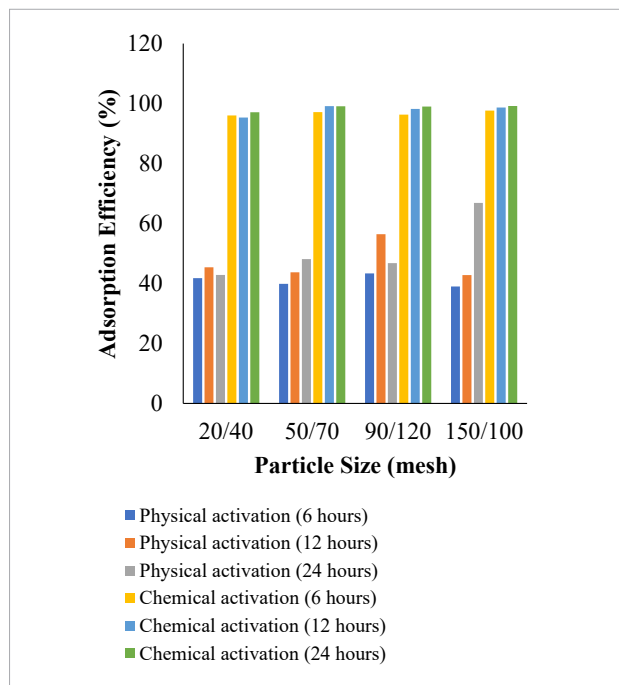
Adsorption efficiency analysis

The values for C_e (adsorbate final concentration after adsorption, ppm) and C_0 (adsorbate concentration

before adsorption, ppm) were obtained through the AAS test on the adsorbate. This adsorption efficiency analysis was obtained using equation 2, presented in Fig. 3.

Fig. 3 shows the effect of cocoa pod husk activated carbon particle size, activation type, and contact time on the Cr(VI) adsorption efficiency. The best result obtained was Cr(VI) adsorption efficiency of 99.20% using chemically activated carbon with a particle size of 150/200 mesh and a contact time of 24 hours. In general, the particle size of the adsorbent material has an inverse relationship with adsorption effectiveness. The greater the overall surface area of the smaller the particles, the greater the capacity to adsorb adsorbates, and the better the adsorption effectiveness (Sajid et al., 2022). This implies that the highest metal adsorption efficiency will occur at the smallest particle size. The chemical activation method is typically more effective because it allows for more uniform pore development and introduces functional groups that aid in adsorption. Meanwhile, physical activation relies more on thermal processes, which can be less effective in creating a highly porous structure compared with chemical activation (Jawad et al., 2017).

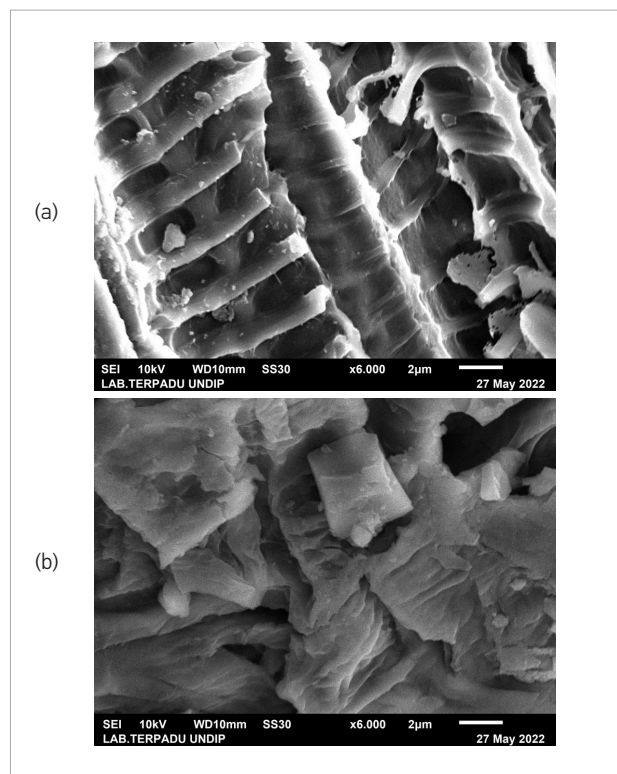
Fig. 3. Results of chromium adsorption efficiency by activated carbon from cocoa pod husk



Scanning electron microscope (SEM) analysis of the best activated carbon

SEM was used to characterize the morphology of the activated carbon physical properties. Fig. 4 shows the surface morphology of cocoa pod husk activated carbon with a particle size of 150/200 mesh magnified 6000 times.

Fig. 4. The surface morphology of cocoa pod husk activated carbon with a particle size of 150/200 mesh (a) before the adsorption process and (b) after the adsorption process with chemical activation and contact time of 24 hours



The selected activated carbon particle size was 150/200 mesh because it had the highest adsorption efficiency value. Fig. 4a shows the surface morphology of cocoa pod husk activated carbon which is hollow, while Fig. 4b illustrates a cross-section of the surface indicating non-hollow carbon porosity. This implies that the adsorbent has the potential to be filled with the Cr(VI) metal during the adsorption process through interaction (Raji et al., 2023). A smaller particle size increases the available surface area to enhance the adsorption process. This is because smaller particles have a larger surface area compared with larger particles (Gora et al., 2022). Therefore, smaller particles have more adsorption sites available to be bound by adsorbates, which can increase the maximum adsorption capacity. This was confirmed by analysis using SEM and AAS.

Conclusions

In conclusion, chemical activation in the manufacture of cocoa pod husk activated carbon provides a higher efficiency value compared with physical activation. The smaller the particle size, the greater the surface area of the particles and the more porosity formed resulting in greater adsorption efficiency. Based on the AAS test, the best adsorption results occurred in the chemically activated 150/200 mesh particle size variation with a contact time of 24 hours. The adsorbed Cr(VI) content was 992.02 ppm with an adsorption efficiency of 99.20%. Additionally, the iodine number of 850.23 mg/g was obtained on activated carbon with a particle size of 150/200 mesh which was also chemically activated. This study proved that cocoa pod husk has potential as activated carbon.

References

- Adiloğlu S., and Göker M. (2021) Phytoremediation: elimination of hexavalent chromium heavy metal using corn (*Zea mays* L.). *Cereal Research Communications* 49(1): 65-72. <https://doi.org/10.1007/s42976-020-00070-9>
- Andrade G. J. C., Quilla J. M. V., Hilares R. T., Meza K. T., Valdivia A. C. M., Aguilar-Pineda J. A., García J. D. C., and Tanaka D. A. P. (2022) Enhanced removal of Bordeaux B and Red G dyes used in alpaca wool dyeing from water using iron-modified activated carbon. *Water (Switzerland)* 14(15): 1-17. <https://doi.org/10.3390/w14152321>
- Arslan H., Eskikaya O., Bilici Z., Dizge N., and Balakrishnan D. (2022) Comparison of Cr(VI) adsorption and photocatalytic reduction efficiency using leonardite powder. *Chemosphere* 300: 1-10. <https://doi.org/10.1016/j.chemosphere.2022.134492>
- Bouzidi A., Djedid M., Ad, C., Benalia M., Hafez B., and Elmsellem H. (2021) Biosorption of Co (II) ions from aqueous solutions using selected local *Luffa Cylindrica*: Adsorption and characterization studies. *Moroccan Journal of Chemistry* 9(1): 156-167.
- Bouzid T., Grich A., Naboulsi A., Regti A., El Himri M., and El Haddad M. (2024) Optimizing Eriochrome Black T adsorption

- through In-Situ polymerization of Poly(aniline-co-formaldehyde) on biochar: Multivariate approach using full factorial Design, Box-Behnken, Artificial intelligence, and DFT. *Separation and Purification Technology* 351. <https://doi.org/10.1016/j.seppur.2024.128107>
- Briffa J., Sinagra E., and Blundell R. (2020) Heavy metal pollution in the environment and their toxicological effects on humans. *Heliyon* 6(9): 1-26. <https://doi.org/10.1016/j.heliyon.2020.e04691>
- Brishti R. S., Kundu R., Habib Md. A., and Ara M. H. (2023) Adsorption of iron(III) from aqueous solution onto activated carbon of a natural source: Bombax ceiba fruit shell. *Results in Chemistry* 5: 1-6. <https://doi.org/10.1016/j.rechem.2022.100727>
- Budaraga I. K., and Putra D. P. (2020) Characteristics of the liquid chemical properties of cocoa skin [*Theobroma cacao* L.] in different water levels. In: *IOP Conference Series: Earth and Environmental Science* (Vol. 497). IOP Publishing Ltd. <https://doi.org/10.1088/1755-1315/497/1/012016>
- Chai W. S., Cheun J. Y., Kumar P. S., Mubashir M., Majeed Z., Banat F., Ho, S. H., and Show P. L. (2021) A review on conventional and novel materials towards heavy metal adsorption in wastewater treatment application. *Journal of Cleaner Production* 296: 1-16. <https://doi.org/10.1016/j.jclepro.2021.126589>
- Chen B., Chen Y., Xu L., Zhang Y., and Li H. (2020) Research and development on industrial heavy metal wastewater treatment technology. In: *IOP Conference Series: Earth and Environmental Science* (Vol. 585). IOP Publishing Ltd. <https://doi.org/10.1088/1755-1315/585/1/012051>
- Chimi T., Hannah B. U., Lincold N. M., Jacques M. B., Tome S., Hermann D. T., Shikuku V. O., Bissoue A. N., Tchieta G. P., and Meva F. E. (2023) Preparation, characterization and application of H₃PO₄-activated carbon from *Pentaclethra macrophylla* pods for the removal of Cr(VI) in aqueous medium. *Journal of the Iranian Chemical Society* 20(2): 399-413. <https://doi.org/10.1007/s13738-022-02675-9>
- El Nemr A., Aboughaly R. M., El Sikaily A., Masoud M. S., Ramadan M. S., and Ragab S. (2022) Microporous-activated carbons of type I adsorption isotherm derived from sugarcane bagasse impregnated with zinc chloride. *Carbon Letters* 32(1): 229-249. <https://doi.org/10.1007/s42823-021-00270-1>
- Fang Y., Li R., Chu Z., Zhu K., Gu F., and Zhang Y. (2020) Chemical and flavor profile changes of cocoa beans (*Theobroma cacao* L.) during primary fermentation. *Food Science and Nutrition* 8(8): 4121-4133. <https://doi.org/10.1002/fsn3.1701>
- Georgaki M. N., and Charalambous M. (2023) Toxic chromium in water and the effects on the human body: a systematic review. *Journal of Water and Health* 21(2): 205-223. <https://doi.org/10.2166/wh.2022.214>
- Gora E. H., Saldana S. G., Casper L. M., Sijercic V. C., Giza O. A., and Sanders R. L. (2022) Effect of exhausted coffee ground particle size on metal ion adsorption rates and capacities. *ACS Omega* 7(43): 38600-38612. <https://doi.org/10.1021/acsomega.2c04058>
- Haryanto B., Tambun R., Siswarni M. Z., Alexander V., and Sinuhaji T. R. F. (2023) Remediation of contaminated sand by Cd ions with variation operation: Batch and flushing column with foam and without foam of SDS surfactant. *South African Journal of Chemical Engineering* 44: 329-335. <https://doi.org/10.1016/j.sajce.2023.03.004>
- Hasanpour M., and Hatami M. (2020) Application of three dimensional porous aerogels as adsorbent for removal of heavy metal ions from water/wastewater: A review study. *Advances in Colloid and Interface Science* 284: 1-24. <https://doi.org/10.1016/j.cis.2020.102247>
- Heidarinejad Z., Dehghani M. H., Heidari M., Javedan G., Ali I., and Sillanpää M. (2020) Methods for preparation and activation of activated carbon: a review. *Environmental Chemistry Letters* 18: 393-415. <https://doi.org/10.1007/s10311-019-00955-0>
- Herawati A., Herdiansyah G., Rahayu, Supriyadi and Nugraheni G. R. (2023) Evaluation of land suitability for cocoa (*Theobroma cacao* L) in Kebonagung District, Pacitan Regency, East Java, Indonesia. In: *IOP Conference Series: Earth and Environmental Science* (Vol. 1162). Institute of Physics. <https://doi.org/10.1088/1755-1315/1162/1/012010>
- Hsiao C. H., Gupta S., Lee C. Y., and Tai N. H. (2023) Effects of physical and chemical activations on the performance of biochar applied in supercapacitors. *Applied Surface Science* 610: 1-10. <https://doi.org/10.1016/j.apsusc.2022.155560>
- Husien S., El-taweel R. M., Salim A. I., Fahim I. S., Said L. A., and Radwan A. G. (2022) Review of activated carbon adsorbent material for textile dyes removal: Preparation, and modelling. *Current Research in Green and Sustainable Chemistry* 5: 1-15. <https://doi.org/10.1016/j.crgsc.2022.100325>
- Jawad A. H., Abd Rashid R., Ismail K., and Sabar S. (2017) High surface area mesoporous activated carbon developed from coconut leaf by chemical activation with H₃PO₄ for adsorption of methylene blue. *Desalination and Water Treatment* 74: 326-335. <https://doi.org/10.5004/dwt.2017.20571>
- Kakom S. M., Abdelmonem N. M., Ismail I. M., and Refaat A. A. (2023) Activated carbon from sugarcane bagasse pyrolysis for heavy metals adsorption. *Sugar Tech* 25(3): 619-629. <https://doi.org/10.1007/s12355-022-01214-3>
- Khait S. A., Kareem E. T., and Shaheed I. M. (2023) Eco-friendly synthesized of CuO nanoparticles using *Anchusa strigosa* L. flowers and study its adsorption activity. *Baghdad Science Journal* 20(4): 1322-1330. <https://doi.org/10.21123/bsj.2023.7444>
- Kuroki A., Hiroto M., Urushihara Y., Horikawa T., Sotowa K. I., and Avila J. R. A. (2019) Adsorption mechanism of metal ions on activated carbon. *Adsorption* 25(6): 1251-1258. <https://doi.org/10.1007/s10450-019-00069-7>

- Mariana M., HPS A. K., Mistar E. M., Yahya E. B., Alfatah T., Danish M., and Amayreh M. (2021) Recent advances in activated carbon modification techniques for enhanced heavy metal adsorption. *Journal of Water Process Engineering* 43: 102221. <https://doi.org/10.1016/j.jwpe.2021.102221>
- Matsedisho B., Otieno B., Kabuba J., Leswif T., and Ochieng A. (2024) Removal of Ni(II) from aqueous solution using chemically modified cellulose nanofibers derived from orange peels. *International Journal of Environmental Science and Technology*. <https://doi.org/10.1007/s13762-024-05819-x>
- Meftah K., Meftah S., Lamkhanter H., Bouzid T., Rezzak Y., Touil S., and Abid A. (2024) Extraction and optimization of *Austrocylindropuntia subulata* powder as a novel green coagulant. *Desalination and Water Treatment* 318. <https://doi.org/10.1016/j.dwt.2024.100339>
- Mei D., Liu L., and Yan B. (2023) Adsorption of uranium (VI) by metal-organic frameworks and covalent-organic frameworks from water. *Coordination Chemistry Reviews* 475: 1-23. <https://doi.org/10.1016/j.ccr.2022.214917>
- Mercileen O. L., Patan A. K., and Lakshmi M. V. V. C. (2023) Selection of chemical activating agent for the synthesis of activated carbon from coconut shell for enhanced dye treatment - its kinetics and equilibrium study. *Materials Today: Proceedings* 72: 274-285. <https://doi.org/10.1016/j.matpr.2022.07.290>
- Mishra N. S., Chandra S., and Saravanan P. (2023) Solvent free synthesis of carbon modified hexagonal boron nitride nanorods for the adsorptive removal of aqueous phase emerging pollutants. *Journal of Molecular Liquids* 369: 1-13. <https://doi.org/10.1016/j.molliq.2022.120969>
- Mizhir Alaa. A., Al-Lami H. S., and Abdulwahid A. A. (2022) Kinetic, isotherm, and thermodynamic study of bismarck brown dye adsorption onto graphene oxide and graphene oxide-grafted-poly(n-butyl methacrylate-co-methacrylic acid). *Baghdad Science Journal* 19(1): 132-140. <https://doi.org/10.21123/bsj.2022.19.1.0132>
- Mudoi M. P., Sharma P., and Khichi A. S. (2022) A review of gas adsorption on shale and the influencing factors of CH₄ and CO₂ adsorption. *Journal of Petroleum Science and Engineering* 217: 1-19. <https://doi.org/10.1016/j.petrol.2022.110897>
- Naboulsi A., Bouzid T., Grich A., Regti A., El Himri M., and El Haddad M. (2024) Understanding the column and batch adsorption mechanism of pesticide 2,4,5-T utilizing alginate-biomass hydrogel capsule: A computational and economic investigation. *International Journal of Biological Macromolecules* 275. <https://doi.org/10.1016/j.ijbiomac.2024.133762>
- Noble R. D., and Terry P. A. (2004) Principles of chemical separations with environmental applications. Cambridge University Press. <https://doi.org/10.1017/CBO9780511616594>
- Rabichi I., Sekkouri C., Yaacoubi F. E., Ennaciri K., Izghri Z., Bouzid T., El Fels L., and Baçaoui A. (2024) Experimental and theoretical investigation of olive mill solid waste biochar for vanillic acid adsorption using DFT/B3LYP Analysis. *Water, Air, and Soil Pollution* 235(6). <https://doi.org/10.1007/s11270-024-07183-5>
- Raji Z., Karim A., Karam A., and Khalloufi S. (2023) Adsorption of heavy metals: Mechanisms, kinetics, and applications of various adsorbents in wastewater remediation-A review. *Waste* 1(3): 775-805. <https://doi.org/10.3390/waste1030046>
- Rodríguez-Reinoso F. (2001) Activated carbon and adsorption. *Encyclopedia of Materials: Science and Technology*. <https://doi.org/10.1016/B0-08-043152-6/00005-X>
- Sajid M., Bari S., Rehman M. S. U., Ashfaq M., Guoliang Y., and Mustafa G. (2022) Adsorption characteristics of paracetamol removal onto activated carbon prepared from Cannabis sativum Hemp. *Alexandria Engineering Journal* 61(9): 7203-7212. <https://doi.org/10.1016/j.aej.2021.12.060>
- Sakhiya A. K., Baghel P., Anand A., Vijay V. K., and Kaushal P. (2021) A comparative study of physical and chemical activation of rice straw derived biochar to enhance Zn⁺² adsorption. *Biore-source Technology Reports* 15: 1-10. <https://doi.org/10.1016/j.biteb.2021.100774>
- Waly S. M., El-Wakil A. M., El-Maaty W. M. A., and Awad F. S. (2021) Efficient removal of Pb(II) and Hg(II) ions from aqueous solution by amine and thiol modified activated carbon. *Journal of Saudi Chemical Society* 25(8): 1-11. <https://doi.org/10.1016/j.jscs.2021.101296>
- Wang J., Wang R., Ma J., and Sun Y. (2022) Study on the application of shell-activated carbon for the adsorption of dyes and antibiotics. *Water (Switzerland)* 14(22): 1-18. <https://doi.org/10.3390/w14223752>
- World Population Review (2022) Cocoa Producing Countries 2022. Yuliusman, Bernama A., and Nafisah A. R. (2020) Synthesis and characterization of coffee based-activated carbon with different activation methods. In: *IOP Conference Series: Materials Science and Engineering* (Vol. 742). Institute of Physics Publishing. <https://doi.org/10.1088/1757-899X/742/1/012036>
- Yuli Y., Eka S., Rakiman and Yazmendra R. (2021) Biomass waste of cocoa skin for basic activated carbon as source of eco-friendly energy storage. In: *Journal of Physics: Conference Series* (Vol. 1788). IOP Publishing Ltd. <https://doi.org/10.1088/1742-6596/1788/1/012020>

